Dalton Transactions

The Crystal Chemistry of Plutonium(IV) Borophosphate

Journal:	*Dalton Transactions*
Manuscript ID	DT-ART-03-2023-000747.R2
Article Type:	Paper
Date Submitted by the Author:	17-Jul-2023
Complete List of Authors:	Sigmon, Ginger; University of Notre Dame, Civil & Environmental Engineering & Earth Sciences DiBlasi, Nicole; University of Notre Dame, Civil & Environmental Engineering & Earth Sciences Hixon, Amy; University of Notre Dame, Civil & Environmental Engineering & Earth Sciences

ARTICLE

The Crystal Chemistry of Plutonium(IV) Borophosphate

Ginger E. Sigmon,[a] Nicole A. DiBlasi,[†a] and Amy E. Hixon*[a]

Received 00th January 20xx,
Accepted 00th January 20xx

DOI: 10.1039/x0xx00000x

In this work, we report the synthesis and characterization of a plutonium(IV) borophosphate, $Pu(H_2O)_3[B_2(OH)(H_2O)(PO_4)_3]$ (**1**). The basic building unit of **1** has a B:P ratio of 2:3 with an equal number of BO_4 and PO_4 groups that assemble into 12-membered rings and take on a sheet topology due to presence of hydroxyl groups or a water molecule on one vertex of each BO_4 tetrahedron. This unique borophosphate anion topology is not observed in other members of the borophosphate family; it is the plutonium(IV) metal centers, rather than borate or phosphate groups, that link the sheets to form an extended framework. The presence of boron in **1** was confirmed using single crystal X-ray diffraction, electron microprobe analysis, and infrared spectroscopy. Peaks corresponding to the tetrahedral BO_4^{5-} and tetrahedral PO_4^{3-} anions were all identified in the fingerprint region (500–1500 cm^{-1}) of the infrared spectrum. Additionally, peaks in the higher wavenumber region corresponded to crystalline water and B-OH vibrations, providing further evidence for the water molecules surrounding plutonium in the structure and the protonation of the BO_4 tetrahedron, respectively. This compound represents the first Pu(IV) borophosphate structure and a novel borophosphate anion topology. Furthermore, the long time-frame required for crystallization of **1** and the suspected leaching of boron from the borosilicate vial used during synthesis indicate that **1** could serve as a model for the crystalline materials that are expected to form during the corrosion of vitrified nuclear waste.

Introduction

Borophosphate materials are compounds containing complex anionic structures built from BO_3 or BO_4 groups, PO_4 groups, and their partially protonated species.[1–3] The term borophosphate describes materials in which the borate and the phosphate groups are directly linked through shared vertices, whereas compounds with isolated borate and phosphate groups are denoted as borate-phosphates. Borophosphate compounds are divided into structures containing tetrahedral or mixed coordinated (tetrahedral and trigonal planar) partial structures, making the coordination number of the borate group important.[2] Borophosphate structures can further be described by their partial dimensionality (*D*) as isolated species or clusters (*D* = 0), infinite chains (*D* = 1), layers or sheets (*D* = 2), and frameworks (*D* = 3). Compounds containing mixed coordinated borophosphates tend to have limited dimensionality, yielding only oligomers and chains.[2]

Borophosphate materials are of interest due to their potential applications in optical devices,[4] for biomedical applications,[5] and as a best practice for nuclear waste management.[6] The latter application involves vitrification of high-level nuclear wastes (e.g., liquid effluents from the reprocessing of used nuclear fuel) in a borophosphate or borosilicate matrix and subsequent emplacement in a geologic repository. Phosphate and borophosphate glasses are proposed for wastes that are rich in chromium, strontium, molybdenum, and the actinide elements[6] and, thus, have a complex composition due to the further addition of salts and glass additives. Questions arise regarding the long-term durability of these amorphous nuclear waste glasses, as eventual corrosion and degradation may lead to the formation of partially crystalline materials and uncertain retention of radionuclide components.

Although actinide phosphate[7–12] and actinide borate[13–18] compounds have been thoroughly studied, actinide borophosphate compounds are rare; only five that contain uranium(VI) have been reported in the literature (see Table 1).[19,20] There are currently no reported plutonium borophosphate materials, though Pu(III) phosphates,[21] Pu(III) borates,[22–25] Pu(V) borates,[26] and Pu(VI) borates[13,27] have been described. While the tetravalent actinide compounds $Th_2(BO_4)(PO_4)$ and $U_2(BO_4)(PO_4)$ have borate and phosphate groups,[28,29] they are considered to be borate-phosphate compounds as opposed to borophosphate compounds because the BO_4 and PO_4 polyhedra are isolated from each other.

Herein, we report the synthesis and characterization of the first plutonium borophosphate, $Pu^{IV}(H_2O)_3[B_2(OH)(H_2O)(PO_4)_3]$ (**1**), and compare its crystal chemistry to related compounds.

[a] *Department of Civil & Environmental Engineering & Earth Sciences, University of Notre Dame, Notre Dame, IN 46556 USA*
[†] Present address: Actinide Analytical Chemistry, Los Alamos National Laboratory, Los Alamos, NM 87545 USA
* Corresponding author e-mail: ahixon@nd.edu
Electronic Supplementary Information (ESI) available: crystal parameters and structural refinement, displacement parameters, anisotropic atomic displacement parameters, selected interatomic distances, bond valence calculations, solid-state absorption spectrum, electron microprobe analysis. See DOI: 10.1039/x0xx00000x

Table 1. Members of the actinide borophosphate family.

Notation	Chemical Formula	*D*	B:P in Building Unit	Reference
AgNBPU-1	$Ag_2(NH_4)_3[(UO_2)_2\{B_3O(PO_4)_4(PO_4H)_2\}]H_2O$	2	1:2	Wu et al.[19]
AgNPBU-2	$Ag_{(2-x)}(NH_4)_3[(UO_2)_2\{B_2P_5O_{(20-x)}(OH)_x\}]$ (x = 1.26)	3	2:5	Wu et al.[19]
AGNBPU-3	$Ag_{(2-x)}(NH_4)_3[(UO_2)_2\{B_2P_{(5-y)}As_yO_{(20-x)}(OH)_x\}]$ (x = 1.43, y = 2.24)	3	2:5	Wu et al.[19]
KUPB1	$K_5(UO_2)_2[B_2P_3O_{12}(OH)]_2(OH)(H_2O)_2$	3	2:3	Hao et al.[20]
KUPB2	$K_2(UO_2)_{12}[B(H_2PO_4)_4](PO_4)_8(OH)(H_2O)_6$	3	1:4	Hao et al.[20]
1	$Pu(H_2O)_3[B_2(OH)(H_2O)(PO_4)_3]$	2	2:3	This work

Experimental Methods

CAUTION: Plutonium is radioactive and should only be handled by trained workers in approved facilities! These experiments were conducted in a laboratory licensed by the U.S. Nuclear Regulatory Commission and the University of Notre Dame Radiation Control Committee. The laboratory is equipped with HEPA-filtered hoods and gloveboxes that are dedicated to transuranic work. The synthesis and characterization described below were carried out in these hoods or gloveboxes and were only transferred to approved instruments once secured in Infineum™ oil.

Synthesis

A plutonium(VI) working solution was prepared from a stock of weapons-grade Pu(IV) in 2 M HCl. An aliquot of this solution was evaporated to near dryness and allowed to cool for 20 minutes. Once cool, 5 mL of concentrated nitric acid and 1 mL of concentrated perchloric acid were added before heating to dryness. After allowing to cool for 20 minutes, 5 mL of concentrated nitric acid was added and evaporated to dryness. This nitric acid evaporation was repeated four times. The final dry plutonium was dissolved in 1 mL concentrated nitric acid to make a 50 mM solution of Pu(VI). The oxidation state of this working solution was confirmed using UV-vis-NIR spectroscopy.

An aliquot of the Pu(VI) working solution (25 µL) was combined with 25 µL of 30% hydrogen peroxide, 5 µL of 2.4 M potassium hydroxide, and 50 µL of 0.5 M potassium pyrophosphate in a borosilicate glass vial to yield a solution with pH ≈ 11. The vial was covered in paraffin film with holes poked in it and checked regularly for three months. A significant volume of the solution evaporated, but no crystals formed, so the vial was capped and moved to storage. Crystals of $Pu(H_2O)_3[B_2(OH)(H_2O)(PO_4)_3]$ (**1**) were identified after one year when vials in the storage area were being collected for plutonium recovery. At this point, single crystals were collected by hand for X-ray diffraction analysis and other analytical characterization. We are unable to accurately determine the yield of this synthesis due to the drying, isolation, and weighing that is required, which pose additional risks to workers as well as difficulties in manipulating the small quantities of material used in the reaction.

Single crystal X-ray diffraction (XRD)

Single crystal X-ray diffraction analysis was conducted using a Bruker Apex II Quazar diffractometer equipped with a Mo Kα X-ray source at 200 K. The unit-cell parameters were refined by least-squares techniques using the Bruker APEX III software. Data were integrated with the Bruker APEX III software and corrected for Lorentz, polarization, and absorption effects, with the latter done using a semi-empirical method in which SADABS was applied. The structure was solved using the Bruker APEX III software. CSD 2190098 contains the supplementary crystallographic data for this paper. These data can be obtained free of charge via www.ccdc.cam.ac.uk/data_request/cif, by emailing data_request@ccdc.cam.ac.uk, or by contacting the Cambridge Crystallographic Data Centre, 12 Union Road, Cambridge CB2 IEZ, UK (fax: +44 1223 336033).

Electron microprobe (EMP)

A Cameca XS-50 electron microprobe with a four-crystal system (ODPB, TAP, PET, LIF) was used to qualitatively confirm the presence of boron in the structure of **1**. Analyses were performed at an accelerating voltage of 7 kV with a beam current of 100 nA. Boron Kα-line measurements were taken of the crystal for 10 seconds and compared to 2-second measurements of a boron metal standard.

Infrared (ATR-FTIR) and absorption (solid-state UV-vis-NIR) spectroscopies

A Bruker Lumos FTIR microscope was used to collect an IR spectrum of a crystal of **1** in Infineum™ oil from 600–4000 cm^{-1} at 25 °C under ambient atmosphere. A CRAIC QDI 2010 UV-vis-NIR microspectrophotometer was used to collect an absorption spectrum from 400–900 nm at 25 °C under ambient atmosphere. Single crystals of **1** were placed on a glass slide in Infineum™ oil and topped with a glass coverslip. Spectra were collected in transmission mode using a 75 W xenon power supply.

Results and Discussion

Crystal Structure

$Pu(H_2O)_3[B_2(OH)(H_2O)(PO_4)_3]$ (**1**) was obtained by slow evaporation of a solution containing Pu(VI), nitric acid, hydrogen peroxide, potassium hydroxide, and potassium pyrophosphate in a borosilicate glass vial. After many months, pink crystals of **1** formed and crystallized in space group *P*3. The crystal structure of **1** has a heteropolyhedral framework formed by a complex borophosphate sheet topology linked together by $PuO_6(H_2O)_3$ polyhedra (Figure 1). Plutonium occupies a triply-capped trigonal prism (<Pu-O> = 2.42 Å), where the basic prism is formed by oxygen atoms from phosphate tetrahedra and the additional vertices are water molecules (Figure 1 inset). Each PO_4 group is bonded to two Pu atoms, one $BO_3(OH)$ tetrahedron, and one $BO_3(OH_2)$ tetrahedron resulting in P-O bond lengths ranging from 1.49 Å to 1.57 Å.

The basic building unit of the borophosphate sheet topology is composed of two borate tetrahedra and three phosphate tetrahedra (Figure 2B). Bond valence sum analyses (Table S5) show that one borate tetrahedron is protonated to form $BO_3(OH)$ and the other is terminated by water to form $BO_3(OH_2)$; the hydroxyl and water molecules are also needed to make the structure charge neutral. Borate and phosphate tetrahedra are linked in an alternating manner (e.g., BO_4-PO_4-BO_4-PO_4) to form an unbranched 12-membered ring. The rings are then further linked through phosphate tetrahedra to form the complex borophosphate sheet topology shown in Figure 2A.

An extended network of 12-membered rings is a typical building unit for compounds with borophosphate framework topologies. For example, the $^3_\infty[BP_2O_8]^{3-}$ 3D anionic framework has been observed in $KMBP_2O_8$ (M = Sr, Ba),[30] $RbPbBP_2O_8$,[31] and $RbBaBP_2O_8$.[32] The borophosphate tetrameric building units within these compounds contain only BO_4 tetrahedra; the BO_4 oxygen atoms are shared with PO_4 tetrahedra in order to connect the 12-membered rings into a framework. In contrast, the 12-membered rings found in **1** take on a sheet topology because there is a hydroxyl group or water molecule on one vertex of each BO_4 tetrahedron.

The borophosphate sheet topology in **1** is not observed in other members of the actinide borophosphate family. Rather, boron and phosphate polyhedra are known to form finite

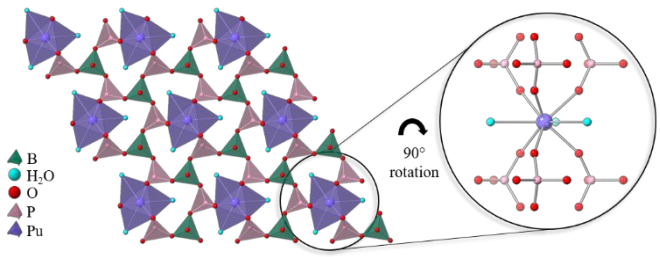

Figure 1. Polyhedral representation of $Pu(H_2O)_3[B_2(OH)(H_2O)(PO_4)_3]$ (**1**) and ball-and-stick model showing the local coordination environment of plutonium. Colors: purple = plutonium polyhedra, pink = phosphorus polyhedra, green = boron polyhedra, red = oxygen atoms, and blue = oxygen atoms from water. Oxygen atoms are of arbitrary size to emphasize the coordination environments of Pu, P, and B.

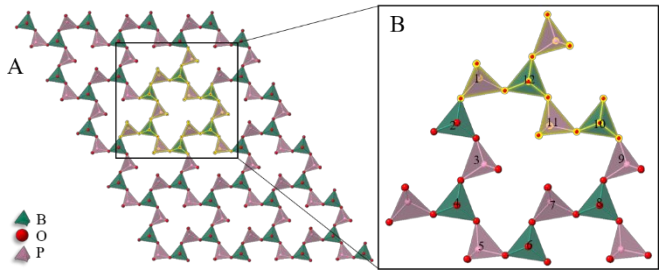

Figure 2. The borophosphate sheet topology is composed of a 12-membered ring (highlighted in (A)) that is formed from three basic building units (highlighted in (B)). Colors: pink = phosphorus tetrahedra, green = boron tetrahedra, and red = oxygen atoms. Oxygen atoms are of arbitrary size to emphasize the coordination environments of P and B.

clusters, chains, or wide bands and coordinate with the actinide metal center to form layered structures or frameworks of different topological types.[19,20] The B:P ratios within the repeating building unit of these compounds dictate the structure type that is formed (Figure 3). For example, the isolated anionic group within **KBPU-2** can be represented as an open-branched pentameric group (B:P = 1:4 in Figure 3),[20] while a finite polyborophosphate group (B:P = 1:2 in Figure 3) is present in **AgNBPU-1**;[19] **KBPU-1** is composed of a loop-branched single chain (B:P = 2:3 in Figure 3); **AgNBPu-2** and **AgNBPU-3** are made up of connected open-branched heptamers (B:P = 2:5 in Figure 3).

The B:P building unit ratio is also an important criterion when it comes to classifying borophosphate compounds, as it has a strong influence on the dimensionality of the anions (Figure 4). For example, the uranyl-based borophosphate compounds discussed above contain only tetrahedral borate, have B:P building unit ratios ranging from 1:4 to 2:3, and have partial dimensionalities (*D*)—used to describe the anion topology of a crystal structure—that represent isolated clusters (*D* = 0) or infinite chains (*D* = 1). In contrast, **1** contains a B:P building unit ratio of 2:3 yet forms a sheet topology (*D* = 2). Compound **1** is the first reported 2D borophosphate material with B:P = 2:3.

Characterization

Solid-state UV-vis-NIR spectroscopy and bond valence calculations were used to confirm the oxidation state of plutonium in **1** (see Figure S1 and Table S5, respectively). The characteristic locations and shapes of the absorption peaks are consistent with the Pu(IV)-aquo spectrum,[33] though relative intensities are different than would be expected because the analysis was conducted on a crystal of **1**. Specifically, the intense peak at 469 nm along with its shoulder at 486 nm and the wide peak with two centers at 652 and 679 nm are characteristic for the absorption of the Pu(IV) aquo ion. The bond valence sum on Pu is 4.18 *v.u.*, consistent with assignment of plutonium as Pu(IV). Reduction of Pu(VI) to Pu(IV) was expected due to the presence of hydrogen peroxide in the synthesis.[34]

The presence of boron in the structure was further investigated by electron microprobe analysis. Although present in small percentages, boron was confirmed in the structure via

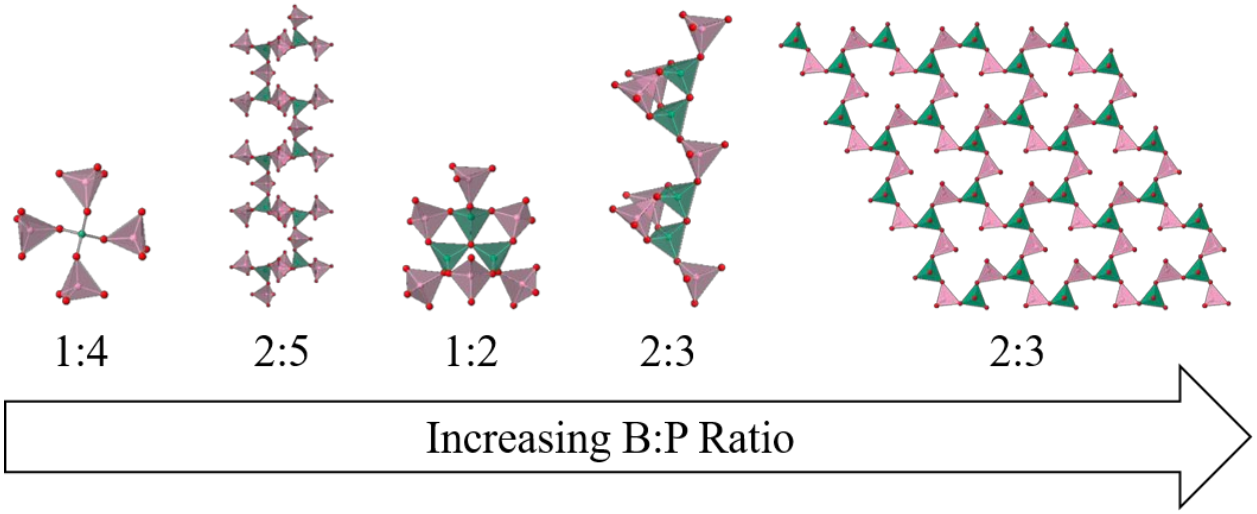

Figure 3. Anion topologies observed within the actinide borophosphate family as a function of B:P building unit ratio. Topologies correspond to the following structures reported in the literature—1:4 = **KBPU-2** $(K_2(UO_2)_{12}[B(H_2PO_4)_4](PO_4)_8(OH)(H_2O)_6)$,[20] 2:5 = **AgNBPU-2** $(Ag_{0.74}(NH_4)_3[(UO_2)_2\{B_2P_5O_{18.74}(OH)_{1.26}\}])$,[19] 1:2 = **AgNBPU-1** $(Ag_2(NH_4)_3[(UO_2)_2\{B_3O(PO_4)_4(PO_4H)_2\}]H_2O)$,[19] 2:3 = **KBPU-1** $(K_5(UO_2)_2[B_2P_3O_{12}(OH)]_{12}(OH)(H_2O)_2)$,[20] 2:3 = **1** $(Pu(H_2O)_3[B_2(OH)(H_2O)(PO_4)_3]$; this work). Colors: pink = phosphorus polyhedra, green = boron atoms or polyhedra, and red = oxygen atoms. Oxygen atoms are of arbitrary size to emphasize the coordination environments of P and B.

comparison with a boron metal standard (Figure S2). The incorporation of boron into **1** was not expected, as no boron was present in the aqueous solution from which **1** crystalized. Instead, we hypothesize that boron leached from the borosilicate vial used during the synthesis. Ongoing experiments are exploring the intentional addition of boron in the synthesis of **1**. It is also possible that the plutonium precursor used in the synthesis contained a boron impurity, as its provenance is unknown.

Attenuated total reflectance Fourier transform infrared spectroscopy (ATR-FTIR) was used to further confirm the presence of boron and phosphate within the structure of **1**. The higher wavenumber region of the FTIR spectrum (Figure 5) shows diatomic interactions. The broad peak from ~3000 to ~3650 cm^{-1} corresponds to molecular water within the lattice and the peak centered at 1618 cm^{-1} corresponds to the δ(HOH) bending of water.[35–39] The sharp peak at 3502 cm^{-1} represents B-OH vibrations while the weak peak at 3355 cm^{-1} likely results from the vibration of crystalline water bonded to plutonium in our structure.[38] This crystal was analyzed using Infineum™ oil, which is also IR active. The three distinct peaks from ~2800 to ~3000 cm^{-1} correspond to the valence vibrations of CH_3 and $(CH_2)_n$-chains in the oil.[41] A fourth peak attributed to the bending vibration of $(CH_2)_n$-chains in the oil is observed at 1463 cm^{-1}.[41] Finally, the CH_2 rocking deformations in the oil is present in the lower wavenumber region at 1369 cm^{-1}.[41] The weak broad peak centered at 2343 cm^{-1} has been identified as a $\nu(CO_2)$ stretch.[42] This contribution is attributed to atmospheric CO_2 and is an artifact of the ATR-FTIR analysis.

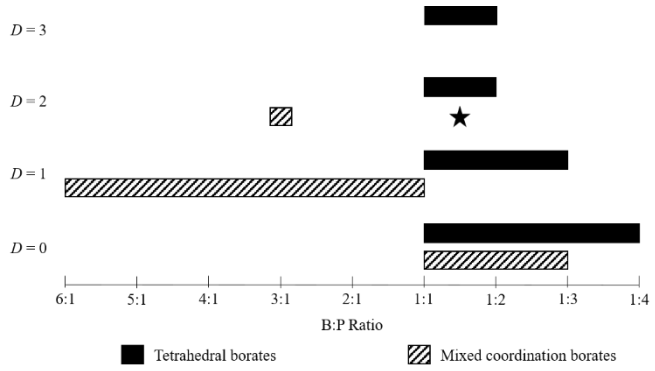

Figure 4. Borophosphate partial structure dimensionality (*D*) as a function of B:P building unit ratio, as established by Ewald et al.[2] and Hasegawa and Yamane.[40] The structure of $Pu(H_2O)_3[B_2(OH)(H_2O)(PO_4)_3]$ (**1**) is denoted by a star.

The fingerprint region of the ATR-FTIR spectrum (500–1500 cm^{-1}) corresponds to vibrational stretching and bending of polyatomic molecules, and thus provides more information regarding the structure of **1**. Because both borate and phosphate anions are strongly IR active within this region, deconvolution and definitive peak identification for this mixed-anion structure is challenging. BO_4^{5-} tetrahedral anions exhibit two IR-active vibrational modes: the stretching mode (ν_3) and the bending mode (ν_4). These have been identified as the peaks at 856 and 611 cm^{-1}, respectively.[35,37,38,43] The peaks at 1272 and 692 cm^{-1} also correspond to a borate vibrational mode and are attributed to in-plane and out-of-plane bending of B-O-H, respectively.[35,37,38,44] For the PO_4^{3-} tetrahedra, the ν_1 symmetric stretching mode and the ν_3 antisymmetric stretching mode have been assigned to the peaks at 978 and 1036 cm^{-1}, respectively.[36,39,45–47] Since our structure contains tetrahedral BO_4^{5-} and PO_4^{3-} anions, it is difficult to differentiate between these within the fingerprint region and determine a single identity for the peaks at 763 and 996 cm^{-1}.

Conclusions

We report the crystallization of $Pu(H_2O)_3[B_2(OH)(H_2O)(PO_4)_3]$ (**1**) from a complex solution in a borosilicate glass vial after one

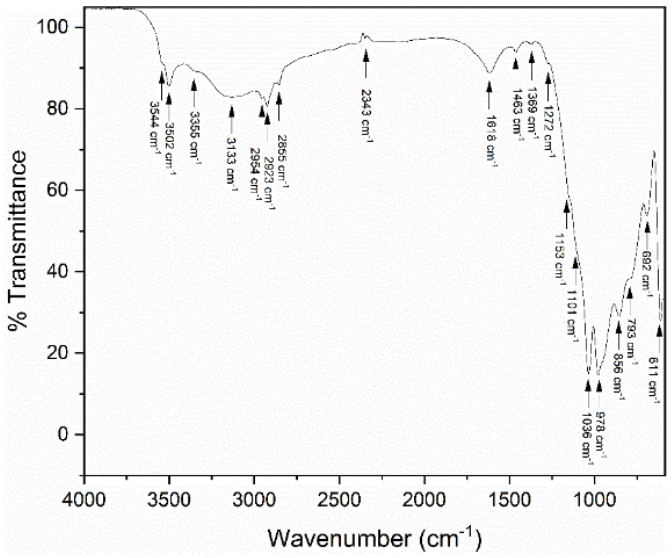

Figure 5. Labelled ATR-FTIR spectrum of $Pu(H_2O)_3[B_2(OH)(H_2O)(PO_4)_3]$ (**1**) in Infineum™ oil.

year. Single crystal X-ray diffraction was used to resolve the crystal structure of **1** and compare the borophosphate anion topology to other members of the actinide borophosphate family. Whereas uranyl-based borophosphates have B:P building unit ratios of 1:4 to 2:3 and 0- or 1-D partial dimensionalities, representing isolated clusters and infinite chains, respectively, **1** had a B:P building unit ratio of 2:3 and a 2-D partial dimensionality. The latter takes the form of a 12-membered ring that forms sheets instead of frameworks due to presence of hydroxyl groups or water molecules on one vertex of each BO_4 tetrahedron. This anion topology is unique across the entire family of borophosphate structures.

A combination of electron microprobe analysis and infrared spectroscopy was used to confirm the presence of boron in the structure of **1** and further characterize additional functional groups, such as phosphate. Peaks corresponding to the tetrahedral BO_4^{5-} and tetrahedral PO_4^{3-} anions were all identified in the fingerprint region (500–1500 cm^{-1}) of the ATR-FTIR spectrum. While it is challenging to deconvolute borate and phosphate anion signals in FTIR, both structural anions must be present to assign each peak in the spectrum. Additionally, peaks in the higher wavenumber region correspond to crystalline water and B-OH vibrations, providing further evidence for the water molecules surrounding plutonium in the structure and the protonation of the BO_4 tetrahedra, respectively.

In conclusion, **1** represents not only the first Pu(IV) borophosphate, but a unique anion topology across the family of borophosphate compounds. It might serve as a model for describing the crystalline aspects of vitrified nuclear waste, but further studies are required to understand its mechanism of formation and solubility, which would control the release of plutonium from vitrified material under field conditions.

Author Contributions

G. Sigmon: conceptualization, methodology, formal analysis, investigation, writing, project administration; N. DiBlasi: conceptualization, methodology, formal analysis, investigation, writing, visualization; A. Hixon: conceptualization, methodology, investigation, resources, writing, visualization, supervision, project administration, funding acquisition

Conflicts of interest

There are no conflicts to declare.

Acknowledgements

The authors thank S. Aksenov for his assistance in solving the initial crystal structure and the ND Energy Materials Characterization Facility for use of the electron microprobe. This material is based on work supported by the Department of Energy, National Nuclear Security Administration as part of the Actinide Center of Excellence under Award Number DE-NA0003763. N. A. DiBlasi was supported by an appointment to the DOE Scholars Program, sponsored by the U.S. Department of Energy and administered by the Oak Ridge Institute for Science and Education, with funding from the Carlsbad Field Office.

References

[1] R. Kniep, H. Engelhardt, C. Hauf, *Chem. Mater.* **1998**, *10*, 2930–2934.
[2] B. Ewald, Y.-X. Huang, R. Kniep, *Z. Für Anorg. Allg. Chem.* **2007**, *633*, 1517–1540.
[3] M. Li, A. Verena-Mudring, *Cryst. Growth Des.* **2016**, *16*, 2441–2458.
[4] G. El Dib, R. Lebullenger, L. Loi, T. Pain, F. Adamietz, L. Canioni, T. Cardinal, S. Chenu, S. Danto, *Opt. Mater.* **2022**, *131*, 112628.
[5] K. Griebenow, in *Phosphate Borate Bioact. Glas.* (Eds.: A. Obata, D.S. Brauer, T. Kasuga), Royal Society Of Chemistry, Croydon, UK, **2022**, pp. 248–262.
[6] Internationale Atomenergie-Organisation, Ed. , *Spent Fuel and High Level Waste: Chemical Durability and Performance under Simulated Repository Conditions: Results of a Coordinated Research Project 1998-2004*, IAEA, Vienna, **2007**.
[7] A. J. Locock, P. C. Burns, *J. Solid State Chem.* **2002**, *163*, 275–280.
[8] A. J. Locock, P. C. Burns, *J. Solid State Chem.* **2002**, *167*, 226–236.
[9] T. Z. Forbes, *Am. Mineral.* **2006**, *91*, 1089–1093.
[10] T. Z. Forbes, P. C. Burns, *Can. Mineral.* **2007**, *45*, 471–477.
[11] E. V. Alekseev, S. V. Krivovichev, T. Malcherek, W. Depmeier, *J. Solid State Chem.* **2008**, *181*, 3010–3015.
[12] E. V. Alekseev, S. V. Krivovichev, W. Depmeier, *J. Solid State Chem.* **2009**, *182*, 2977–2984.
[13] S. Wang, E. V. Alekseev, J. Ling, S. Skanthakumar, L. Soderholm, W. Depmeier, T. E. Albrecht-Schmitt, *Angew. Chem. Int. Ed.* **2010**, *49*, 1263–1266.
[14] M. J. Polinski, S. Wang, E. V. Alekseev, W. Depmeier, G. Liu,

R. G. Haire, T. E. Albrecht-Schmitt, *Angew. Chem. Int. Ed.* **2012**, *51*, 1869–1872.

[15] M. J. Polinski, E. B. G. Iii, R. Maurice, N. Planas, J. T. Stritzinger, T. G. Parker, J. N. Cross, T. D. Green, E. V. Alekseev, S. M. V. Cleve, W. Depmeier, L. Gagliardi, M. Shatruk, K. L. Knappenberger, G. Liu, S. Skanthakumar, L. Soderholm, D. A. Dixon, T. E. Albrecht-Schmitt, *Nat. Chem.* **2014**, *advance online publication*, DOI 10.1038/nchem.1896.

[16] M. J. Polinski, K. A. Pace, J. T. Stritzinger, J. Lin, J. N. Cross, S. K. Cary, S. M. V. Cleve, E. V. Alekseev, T. E. Albrecht-Schmitt, *Chem. - Eur. J.* **2014**, *20*, 9892–9896.

[17] S. Wu, S. Wang, M. Polinski, O. Beermann, P. Kegler, T. Malcherek, A. Holzheid, W. Depmeier, D. Bosbach, T. E. Albrecht-Schmitt, E. V. Alekseev, *Inorg. Chem.* **2013**, *52*, 5110–5118.

[18] T. G. Parker, A. L. Chown, A. Beehler, D. Pubbi, J. N. Cross, T. E. Albrecht-Schmitt, *Inorg. Chem.* **2015**, *54*, 570–575.

[19] S. Wu, M. J. Polinski, T. Malcherek, U. Bismayer, M. Klinkenberg, G. Modolo, D. Bosbach, W. Depmeier, T. E. Albrecht-Schmitt, E. V. Alekseev, *Inorg. Chem.* **2013**, *52*, 7881–7888.

[20] Y. Hao, G. L. Murphy, D. Bosbach, G. Modolo, T. E. Albrecht-Schmitt, E. V. Alekseev, *Inorg. Chem.* **2017**, *56*, 9311–9320.

[21] K. Popa, P. E. Raison, L. Martel, P. M. Martin, D. Prieur, P. L. Solari, D. Bouëxière, R. J. M. Konings, J. Somers, *J. Solid State Chem.* **2015**, *230*, 169–174.

[22] M. J. Polinski, S. Wang, E. V. Alekseev, W. Depmeier, T. E. Albrecht-Schmitt, *Angew. Chem. Int. Ed.* **2011**, *50*, 8891–8894.

[23] S. Wang, E. V. Alekseev, W. Depmeier, T. E. Albrecht-Schmitt, *Inorg. Chem.* **2011**, *50*, 2079–2081.

[24] M. J. Polinski, D. J. Grant, S. Wang, E. V. Alekseev, J. N. Cross, E. M. Villa, W. Depmeier, L. Gagliardi, T. E. Albrecht-Schmitt, *J. Am. Chem. Soc.* **2012**, *134*, 10682–10692.

[25] M. J. Polinski, S. Wang, J. N. Cross, E. V. Alekseev, W. Depmeier, T. E. Albrecht-Schmitt, *Inorg. Chem.* **2012**, *51*, 7859–7866.

[26] T. K. Deason, A. T. Hines, G. Morrison, M. D. Smith, T. M. Besmann, A. M. Mofrad, F. F. Fondeur, I. Lehman-Andino, J. W. Amoroso, D. P. DiPrete, H.-C. zur Loye, *J. Am. Chem. Soc.* **2023**, *145*, 10007–10014.

[27] S. Wang, E. M. Villa, J. Diwu, E. V. Alekseev, W. Depmeier, T. E. Albrecht-Schmitt, *Inorg. Chem.* **2011**, *50*, 2527–2533.

[28] C. Lipp, P. C. Burns, *Can. Mineral.* **2011**, *49*, 1211–1220.

[29] E. Hinteregger, K. Wurst, L. Perfler, F. Kraus, H. Huppertz, *Eur. J. Inorg. Chem.* **2013**, *2013*, 5247–5252.

[30] D. Zhao, W.-D. Cheng, H. Zhang, S.-P. Huang, Z. Xie, W.-L. Zhang, S.-L. Yang, *Inorg. Chem.* **2009**, *48*, 6623–6629.

[31] Y. Wang, S. Pan, M. Zhang, S. Han, X. Su, L. Dong, *CrystEngComm* **2013**, *15*, 4956–4962.

[32] M. A. Khan, Y.-Y. Li, H. Lin, L.-J. Zhang, P.-F. Liu, H.-J. Zhao, R.-H. Duan, J.-Q. Wang, L. Chen, *J. Solid State Chem.* **2016**, *243*, 259–266.

[33] D. L. Clark, S. S. Hecker, G. D. Jarvinen, M. P. Neu, in *Chem. Actin. Trans. Elem.*, Springer, Dordrecht, The Netherlands, **2006**, pp. 813–1264.

[34] D. L. Clark, D. A. Geeson, R. J. Hanrahan, Jr., Eds. , *Plutonium Handbook*, American Nuclear Society, **2019**.

[35] L. Jun, X. Shuping, G. Shiyang, *Spectrochim. Acta. A. Mol. Biomol. Spectrosc.* **1995**, *51*, 519–532.

[36] K. Nakamoto, *Infrared and Raman Spectra of Inorganic and Coordination Compounds, Part B: Applications in Coordination, Organometallic, and Bioinorganic Chemistry*, John Wiley & Sons, **2009**.

[37] C. Gautam, A. K. Yadav, A. K. Singh, *ISRN Ceram.* **2012**, *2012*, e428497.

[38] B.-C. Zhao, W. Sun, W.-J. Ren, Y.-X. Huang, Z. Li, Y. Pan, J.-X. Mi, *J. Solid State Chem.* **2013**, *206*, 91–98.

[39] I. Korybska-Sadło, M. Sitarz, M. Król, P. Gunia, *Spectrosc. Lett.* **2016**, *49*, 606–612.

[40] T. Hasegawa, H. Yamane, *Dalton Trans.* **2014**, *43*, 14525–14528.

[41] N. V. Chukanov, A. D. Chervonnyi, *Infrared Spectroscopy of Minerals and Related Compounds*, Springer, **2016**.

[42] J. M. Chalmers, in *Handb. Vib. Spectrosc.*, John Wiley & Sons, Ltd, **2006**.

[43] C. E. Weir, R. A. Schroeder, *J. Res. Natl. Bur. Stand. Sect. Phys. Chem.* **1964**, *68A*, 465.

[44] R. L. Frost, Y. Xi, R. Scholz, F. M. Belotti, M. Cândido Filho, *J. Mol. Struct.* **2013**, *1037*, 23–28.

[45] F. A. Miller, C. H. Wilkins, *Anal. Chem.* **1952**, *24*, 1253–1294.

[46] H. H. Adler, *Am. Mineral.* **1964**, *49*, 1002–1015.

[47] L. C. Thomas, R. A. Chittekden, *Spectrochim. Acta Part Mol. Spectrosc.* **1970**, *26*, 781–800.